Journal of Applied Mechanics Vol.7,pp.97-107 (August 2004) JSCE

Modified damage identification algorithm based on vibration measurements

振動計測に基づく損傷同定アルゴリズムの改良

Sherif Beskhyroun*, Shuichi Mikami**, Tomoyuki Yamazaki *** and Toshiyuki Oshima****
シェリフ ベスキロウン*, 三上修一**, 山崎智之***, 大島俊之****

*Doctoral Student, Dept. of Civil Eng., Kitami Institute of Technology, (165 Koen-cho, Kitami, 090-8507)
**Associate Professor, Dept. of Civil Eng., Kitami Institute of Technology, (165 Koen-cho, Kitami, 090-8507)
***Research Associate, Dept. of Civil Eng., Kitami Institute of Technology, (165 Koen-cho, Kitami, 090-8507)
****Professor, Dept. of Civil Eng., Kitami Institute of Technology, (165 Koen-cho, Kitami, 090-8507)

In this paper, a newly derived algorithm to detect damage and predict its location in structures using changes in vibration measurements is presented. First, an existing algorithm of damage detection is reviewed and the new algorithm is formulated in order to detect damage and improve the accuracy of damage localization using low frequency range. Compared to the existing damage detection algorithm, the new algorithm showed the ability to detect and localize damage more accurately using very low frequency range without the need for measuring higher modes.

Key Words: damage detection, modal parameters, vibration data, health monitoring

1. Introduction

Structural systems are susceptible to structural damage over their operating lives from impact, operating loads, and fatigue. Identifying the location of structural damage leads to improved safety and offers the possibility of extending the service life of a structure by repairing structure components when necessary. Therefore, the ability to monitor a structure and detect damage at the earliest possible stage is becoming increasingly important. Many damage detection schemes rely on analyzing response measurements from sensors placed on the structure[1-5]. Damage-detection methods such as acoustic or ultrasonic methods, magnetic field methods, radiograph, eddy-current methods and thermal field methods are either visual or localized experimental methods[6,7]. It is difficult to apply these methods to detect damage in large structures or inaccessible members. Therefore there is a need for more global damage detection methods that can be applied to complex structure. During the past decade, a significant amount of research has been conducted in the area of damage detection using the dynamic response of a structure. Research efforts have been made to detect structural damage directly from dynamic response measurements in the time domain, e.g., the random decrement technique[8,9], or from frequency response functions (FRF)[10]. Also, methods have been proposed to detect damage using system identification techniques[11,12]. Many studies have been conducted in the area of non-destructive damage detection (NDD) using changes in modal parameters. Researches have related changes in natural frequencies, mode shapes and damping to changes in beam properties such as cracks, notches or changes in boundary conditions. Damage Index Method[13] is one of the most referenced methods for detecting and localizing damage in beam type structures using changes in mode shapes. In many structures only few modes are available which may decrease the accuracy of detecting and localizing damage using this method. In this paper, a proposed algorithm based on this method is presented which uses magnitudes of Cross Spectral Density (CSD) instead of using mode shapes. The advantage of using CSD magnitude is that a lower range of frequency can be used without the need for measuring higher modes. The second advantage is that CSD is calculated from the displacement or acceleration response between every channel relative to one reference channel without measuring the excitation force. Therefore, ambient vibration can be used as an excitation force for continuous health monitoring of structures. The proposed algorithm provides a method that reduces false positive readings and hence increases the accuracy of localizing damage position.

The proposed algorithm presented here and Damage Index Method will be applied using experimental and numerical data

¶ Dedicated to the memory of Prof. Michihiro KITAHARA

extracted from simple steel beam after making one and multiple cracks. Both algorithms are evaluated by detecting damage and predicting its location. The performance of each algorithm is assessed by quantifying the accuracy of damage prediction results. In the structure of interest in this study, the objective is to detect low magnitude damage at a very early stage using low frequency range (few available mode shapes). In such cases, changes in modal parameters between the undamaged and damaged structures are small and the application of CSD magnitude can provide a reliable means of detecting and localizing damage.

2. Experiment setup and equipments

In this research, a simple steel beam supported by four bolts in both sides was examined before and after inducing some cracks, as shown in Fig. 1. The multi-layer piezoelectric actuator is used for local excitation. The main advantage of using piezoelectric actuator is that it produces vibration with different frequencies ranging from 0 to 400 Hz that is effective in measuring mode shapes[14]. Seven accelerometers were positioned on the top flange and one accelerometer was used as a reference channel, as shown in Fig. 2. It was noticed that changing the location of the reference channel did not affect on the results obtained from the studied methods. A polynomial can be fit to the modal data (mode shapes or CSD magnitudes) and then subsequently differentiated to obtain the curvature values. Interpolation procedures can be used to generate additional degrees of freedom at locations between sensors, which can increase the accuracy of locating damage between sensors. When cubic polynomial function was used to fit the modal data, better results in detecting and locating damage were obtained than using spline interpolation scheme. The cubic polynomial function was used to fit CSD magnitude (or mode shape amplitude) between the seven accelerometers. Therefore, the total distance between accelerometers is divided into 120 nodes (Fig. 2). Two cases of damage were introduced to the beam. Case 1 of damage was simulated by inducing one crack, 2 x 40 mm, at node 40 and Case 2 of damage was simulated by inducing 2 cracks with the same previous dimensions at nodes 40 and 90, as shown in Fig. 2.

3. Damage identification methods

3.1 Damage Index method

Damage Index Method[13] is used to detect and locate damage in structures using mode shapes before and after damage. For a structure that can be represented as a beam, a damage index β is developed based on the change in strain energy stored in the structure when it deforms in its particular mode shape. For location j on the beam this change in the i^{th} mode strain energy is related to the change in curvature of the mode at location j. The damage index for this location and this mode, β_{ij}, is defined as

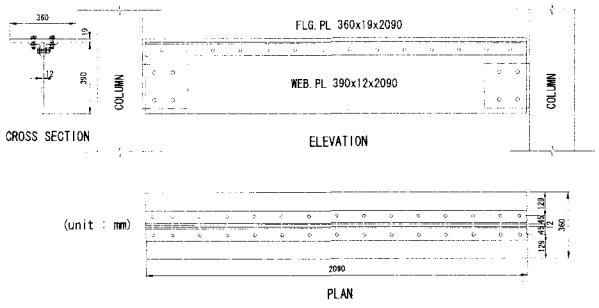

Fig. 1 Beam dimensions

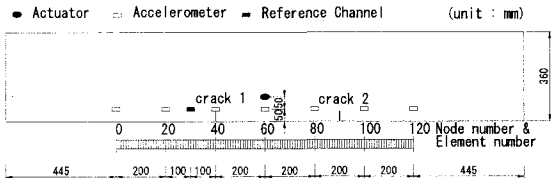

Fig. 2 Actuator and accelerometers positions and element numbers

$$\beta_{ij} = \frac{(\int_a^b [\psi_i^{*''}(x)]^2 dx + \int_0^L [\psi_i^{*''}(x)]^2 dx)\int_0^L [\psi_i''(x)]^2 dx}{(\int_a^b [\psi_i''(x)]^2 dx + \int_0^L [\psi_i''(x)]^2 dx)\int_0^L [\psi_i^{*''}(x)]^2 dx} \quad (1)$$

where $\psi''(x)$ $\psi^{*''}(x)$ are the second derivative of i^{th} mode shape corresponding to the undamaged and damaged structure, respectively. L is beam length and a, b are the limits for element j. When more than one mode is used, damage index is defined as the sum of damage indices from each mode as follows

$$\beta_j = \sum_{i=1}^{n} \beta_{ij} \quad (2)$$

where n is the number of modes. Peak value of β_j indicates damage at element j.

3.2 Proposed algorithm

In the modified algorithm presented here, the magnitude of Cross Spectral Density at each frequency will be used instead of using mode shapes. CSD is calculated from displacement or acceleration response at each channel relative to one reference channel. At each frequency value, f, the magnitude of CSD at channel i can be calculated from the real and imaginary values as follows

$$\psi_{if} = \sqrt{\mathrm{Re}(f)^2 + \mathrm{Im}(f)^2} \quad (3)$$

$\{\psi_f\}$ is a vector representing CSD magnitudes at all measured points at the same frequency, f_i. Before analyzing CSD data with any damage identification routine, the CSD data has to be first normalized. There are several approaches in which to normalize the CSD data. For this problem, the approach taken is to normalize the CSD magnitudes at each frequency with respect to the square root of the sum of squares (SRSS) as shown in the following expression

$$\{\phi_f\} = \frac{1}{\sqrt{\sum_{i=1}^{p} \psi_{if}^2}} \{\psi_f\} \tag{4}$$

where $\{\phi_f\}$ = the normalized CSD magnitudes, $\{\psi_f\}$ represent the original CSD magnitudes at frequency f gathered experimentally or analytically, p = the number of measured points, and ψ_{if} represents CSD magnitude at channel i at frequency f.

Interpolation using cubic polynomial function is carried out to approximate CSD magnitude between sensors. Thus, $\phi_f(x)$ represents the normalized magnitude of CSD at distance x at frequency f after interpolation.

Similar to Eq. (1), new damage index can be calculated using the magnitude of CSD as follows

$$\alpha_{f,j} = \frac{(\int_a^b [\phi_f^{*''}(x)]^2 dx + \int_0^L [\phi_f^{*''}(x)]^2 dx) \int_0^L [\phi_f''(x)]^2 dx}{(\int_a^b [\phi_f''(x)]^2 dx + \int_0^L [\phi_f''(x)]^2 dx) \int_0^L [\phi_f^{*''}(x)]^2 dx} \tag{5}$$

where $\phi_f''(x)$ $\phi_f^{*''}(x)$ are the second derivative of CSD magnitude at frequency f corresponding to the undamaged and damaged structure, respectively. L is beam length and a, b are the limits for element j. Assuming that the collection of the damage indices, $\alpha_{f,j}$, represents a sample population of a normally distributed random variable, a normalized damage indicator is obtained as follows

$$Q_{f,j} = \frac{\alpha_{f,j} - \overline{\alpha_f}}{\sigma_f} \tag{6}$$

where $\overline{\alpha_f}$ and σ_f represent the mean and standard deviation of the damage indices, respectively and defined as follows

$$\overline{\alpha_f} = \sum_{j=1}^{NE} \alpha_{f,j} \Big/ NE \tag{7}$$

$$\sigma_f = \sqrt{\sum_{j=1}^{NE} (\alpha_{f,j} - \overline{\alpha_f})^2} \Big/ (NE - 1) \tag{8}$$

where NE = number of elements after interpolation

A statistical decision making procedure is employed to determine if the normalized damage index, $Q_{f,j}$, is associated with a damage location. Values of four standard deviations from the mean are assumed to be associated with damage locations. Different scenarios of damage (different sizes and different locations) were introduced to the numerical model and it was found that using value of four as a limit to identify the damage location gives the best results. Using values less than four will increase the possibility of false positive readings and values bigger than four will decrease the ability to detect small damage. In Eq. (5), it is assumed that CSD curvature will change due to damage significantly at the damaged locations and slightly near to the damaged zone (undamaged locations). Therefore, it is expected that $Q_{f,j}$ will have bigger values at the damaged locations and smaller values at the undamaged locations. The sum of these small values of $Q_{f,j}$ at the undamaged locations may deteriorate the actual position of damage and create false positive readings. Therefore, in order to reduce the effect of false positive readings, $Q_{f,j}$ values less than four are removed and values greater than or equal to four are added over different frequencies on the measurement range, as shown in the following expressions

$$\text{if } |Q_{f,j}| < 4 \text{ then let } Q_{f,j} = 0 \text{ and } L_{f,j} = 0 \tag{9}$$

$$\text{if } |Q_{f,j}| \geq 4 \text{ then let } Q_{f,j} = Q_{f,j} \text{ and } L_{f,j} = 1 \tag{10}$$

When normalized damage index, $Q_{f,j}$, is calculated using the magnitude of CSD at different frequencies on the measurement range from $F1$ *to* $F2$, the new damage index is defined as the sum of absolute values of damage indices measured at different frequencies as follows

$$S_j = \sum_{f=F1}^{F2} |Q_{f,j}| \tag{11}$$

$L_{f,j}$ is used as a counter to identify the number of times damage is detected at element number j. The sum of $L_{f,j}$ over the different frequencies on the measurement range gives the total number of times damage is detected at element j as follows

$$O_j = \sum_{f=F1}^{F2} L_{f,j} \tag{12}$$

The product of damage index, S_j, and the total number of times, O_j, defines the accumulated damage indicator, DI_j

$$DI_j = S_j O_j \tag{13}$$

4. Experimental measurements

4.1 Measurement of Cross Spectral Density

Fig. 3 shows CSD between channel 3 and the reference channel for the intact beam. The test was repeated four times and significant changes in CSD were noticed in some frequency range before making any damage, a typical example was from 10 to 150 Hz. On the other hand, there were other frequency ranges where no significant change in CSD was noticed, even after repeating the test four times. Example of these, were from 175 to 225 Hz and from 270 to 350 Hz. The same remarks were also observed in the damaged beam. Based on these observations, it is very important to choose the frequency range in which change in CSD is due to damage not because of noise or measurement errors. Fig. 4 shows the comparison between CSD for the intact and damaged beam with one crack. Thin lines indicate CSD for the intact beam and thick lines indicate CSD for the damaged beam, the test was repeated four times for each case. In this figure, change in CSD in the frequency range from 10 to 150 Hz is obviously due to noise or measurement errors and not due to damage. On the other hand, it is clear that change in CSD in the frequency range from 290 to 350 Hz is due to damage. Similar observations were also noticed when two cracks were induced on the

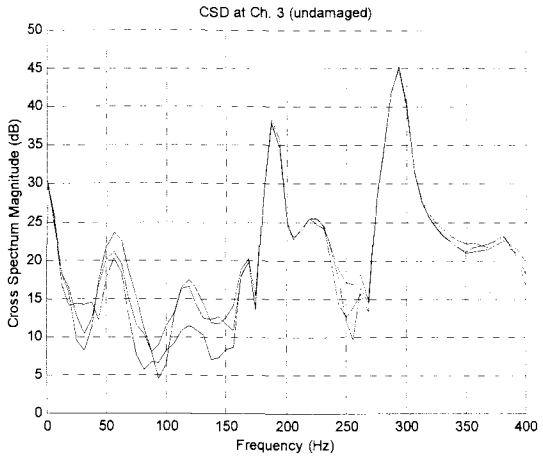

Fig. 3 CSD at channel 3 for the intact beam

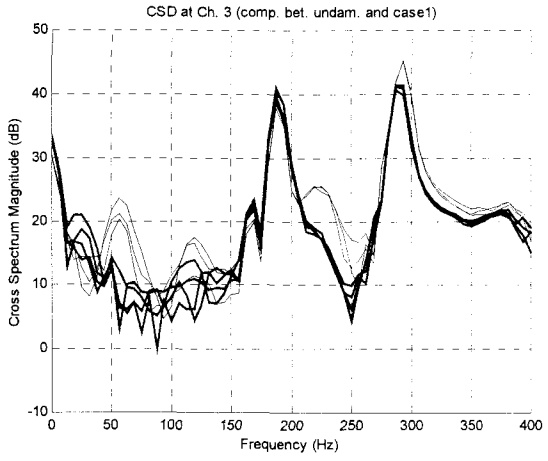

Fig. 4 Comparison bet. CSD for the intact beam and case1 of damage

beam. In order to choose the frequency range in which CSD magnitudes can be used in the proposed damage identification algorithm, the Modal Assurance Criterion (MAC) is used as explained in the following section.

4.2 Choosing measurement range of Cross Spectral Density

Modal Assurance Criterion (MAC)[15] compares two modes using the orthogonality properties of the mode shapes. The MAC that compares mode i and j has the form

$$\mathrm{MAC}(i,j) = \frac{\left|\sum_{k=1}^{n}(\phi_j)_k(\phi_i)_k^*\right|^2}{\left[\sum_{k=1}^{n}(\phi_j)_k(\phi_j)_k^*\right]\left[\sum_{k=1}^{n}(\phi_i)_k(\phi_i)_k^*\right]} \qquad (14)$$

where $(\phi)_k$ is an element of the mode-shape vector and the asterisks denote complex conjugate. In practice, MAC value greater than 0.9 indicates correlated modes and value less than 0.05 indicates uncorrelated modes. MAC is used to compare CSD data obtained from two tests for the undamaged structure in order to determine the frequency range in which CSD is stable. In Eq. (14), CSD magnitudes at frequency f for the first test, $\{\phi_f\}_1$, simulate mode i and CSD magnitudes at the same frequency f but for the second test, $\{\phi_f\}_2$ simulate mode j. At each frequency value, a MAC value close to unity indicates that CSD magnitudes obtained from the two tests are similar or close. On the other hand, a MAC value that is far from unity indicates a great disparity in the CSD magnitudes. In the same manner, MAC can be used to compare CSD magnitudes obtained from the intact structure with CSD magnitudes obtained from the damaged one. In Fig. 5, MAC is used to compare CSD obtained from two different tests carried out on the intact beam. In the frequency range from 10 to 150 Hz, the values of MAC are low which indicate big difference in CSD between the two tests. On the other hand, values of MAC are very close to unity in the frequency range of 307 to 375 Hz, which indicate very stable data and small measurement errors in this range. The same remarks can be observed when CSD for the intact beam is compared to CSD for the beam with one crack, as shown in Fig. 6. In Fig. 7, MAC is used to compare CSD data for the following cases:

(I) Two different tests carried out on the intact beam, indicated by solid line.

(II) Intact beam and damaged beam with one crack, indicated by dashed line.

(III) Intact beam and damaged beam with two cracks, indicated by dot line.

In this figure, it is clear for all three cases that MAC value is close to unity in the frequency range of 307 to 375 Hz. The small and gradual changes in MAC values in that frequency range is another indication of how CSD changes due to damage. Therefore, the CSD magnitudes within the frequency range of 307 to 375 Hz are recommended for the proposed algorithm.

5. Damage identification methods applied to experimental data

The objective here is to evaluate the feasibility of the proposed algorithm to detect and localize damage in an experimental and numerical model of a structure when only data on a few modes of vibration are available. Damage Index Method and the proposed algorithm will be applied to the experimental data to compare the accuracy of both algorithms in detecting and localizing the damage.

5.1 Crack at node 40

(1) Using Damage Index Method

Fig. 8 shows the obtained results when Damage Index Method is applied to experimental data after inducing one crack at node 40. Two mode shapes are measured for the intact and damaged beam. These mode shapes are used to detect damage and predict its position using the existing algorithm (Eq. 1). In this figure, two peak values appear at elements 39 and 99, which indicate damage at these elements. The indicated position at element 39 is accurate but the position at element 99 is false positive reading.

(2) Using the proposed algorithm

CSD magnitudes, for the intact and damaged beam, in the frequency range from 307 to 375 Hz are used in the proposed

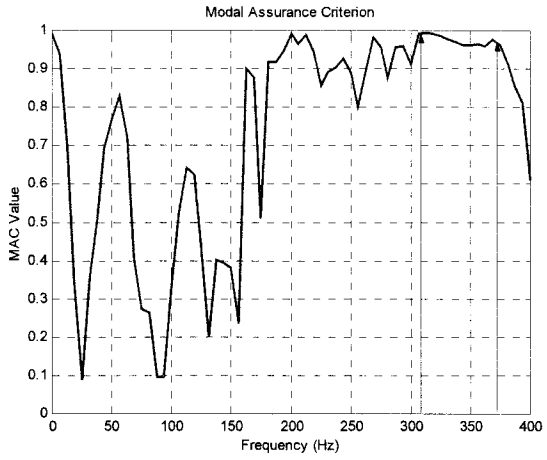

Fig. 5 Comparing CSD data obtained from two different tests for the intact beam using MAC

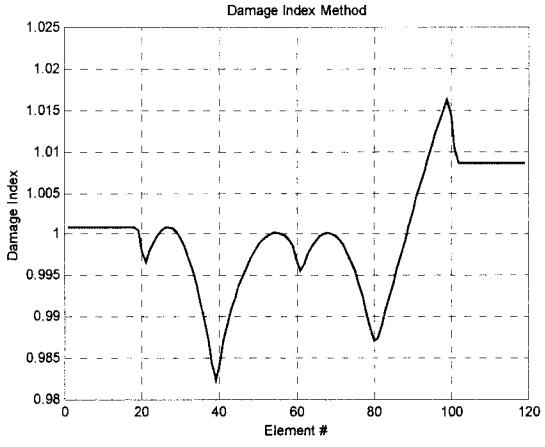

Fig. 8 Damage Index Method applied to experimental data for crack at node 40

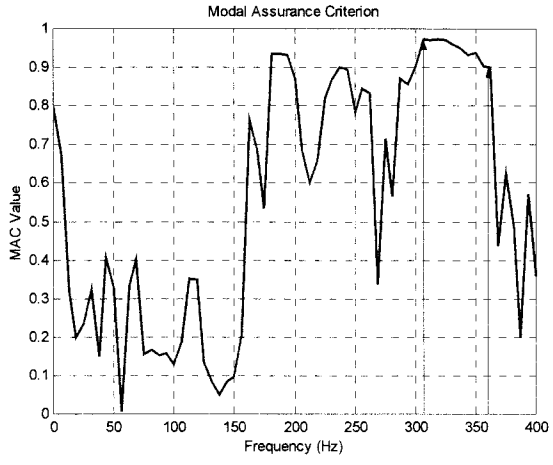

Fig. 6 Comparing CSD data obtained from the intact beam and the beam with one crack using MAC

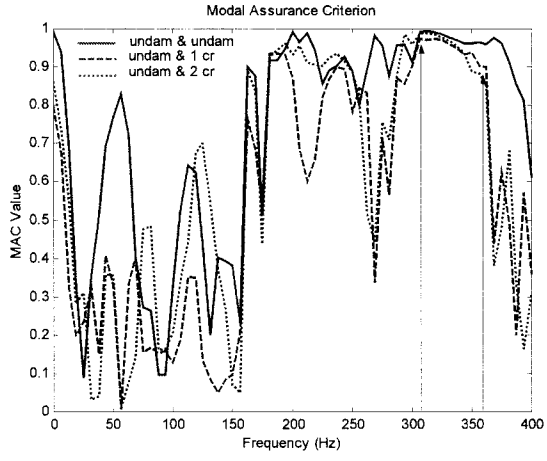

Fig. 7 Comparing CSD data obtained from the intact beam and the beam with different cases of damage using MAC

algorithm. Damage is detected and the location of damage is determined more accurately, as shown in Fig. 9. As clearly indicated in this figure, damage was indicated at element 39 with a small indication of damage at element 41. Furthermore, no false positive readings appeared when the proposed algorithm was applied using that frequency range, from 307 to 375 Hz. Damage was detected and localized very accurately when CSD magnitudes were used in the frequency range from 300 to 400 Hz. However, poor results in localizing the damage position were obtained when CSD magnitudes were used in frequency range from 4 to 400 Hz because noise and measurement errors are high in some frequency ranges, as earlier explained. In the measurement range, CSD magnitude is used at each frequency to detect and locate damage. Damage is detected only at some frequencies within the measurement range not at all frequencies. In order to determine how many times the damage is detected at certain element, O_j in Eq. (12) is plotted. Fig. 10 shows the number of times cracks were detected at each element. Damage at element 39 was detected 4 times ($O_{39} = 4$) and damage at element 41 was detected only once ($O_{41} = 1$).

5.2 Cracks at nodes 40 and 90

In this section, damage identification methods are applied to the experimental data after inducing two cracks at nodes 40 and 90. The main objective here is to demonstrate and compare the feasibility of the proposed algorithm to detect and localize multiple cracks.

(1) Using Damage Index Method

Fig. 11 shows the obtained results when Damage Index Method was applied to detect damage at nodes 40 and 90 using two measured mode shapes. In this figure, three peaks appear at elements 39, 80 and 99, which indicate damage at these elements. Damage at node 40 is indicated accurately and damage at node 90 is indicated between elements 80 and 99. It can be observed that it is due to the sensors being positioned at nodes 0, 20, 40, 60, 80, 100 and 120, the accuracy of damage localization tends to decrease during damage occurrence between sensors. Although the use of cubic polynomial to approximate modal amplitude or CSD magnitude between sensors was not effective in increasing the accuracy of localizing damage between sensors it is, however, useful in obtaining the curvature of modal data or CSD data.

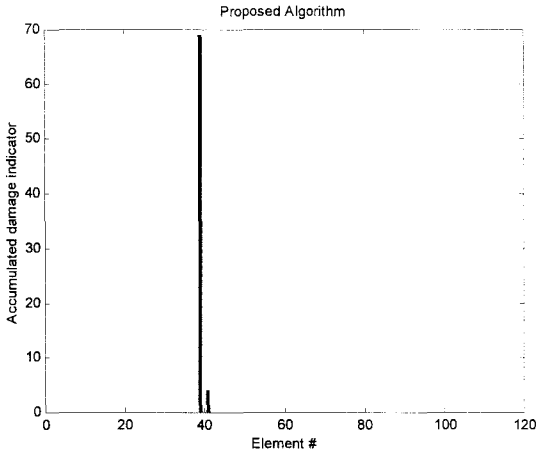

Fig. 9 The proposed algorithm applied to experimental data for crack at node 40 using freq. range from 307 to 375 Hz.

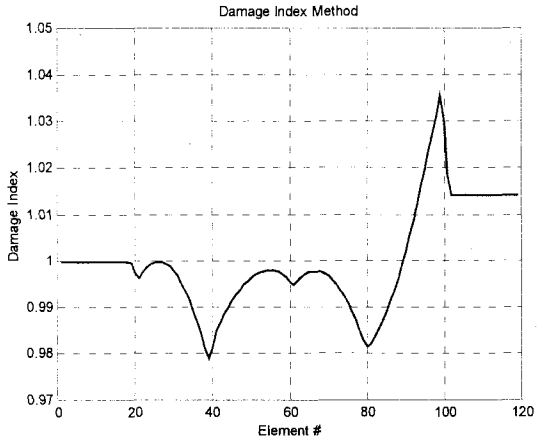

Fig. 11 Damage Index Method applied to experimental data for cracks at nodes 40 and 90

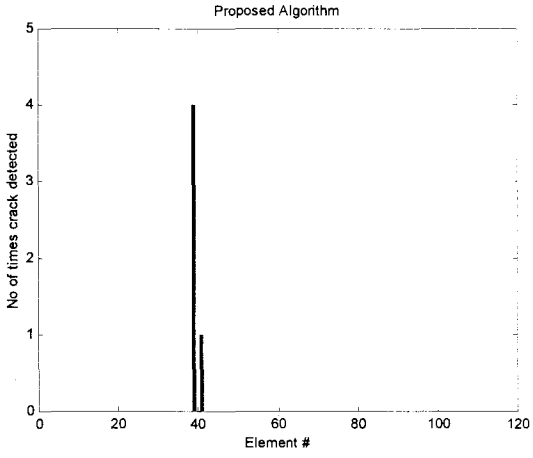

Fig. 10 Number of times cracks detected in experimental data for crack at node 40 using freq. range from 307 to 375 Hz.

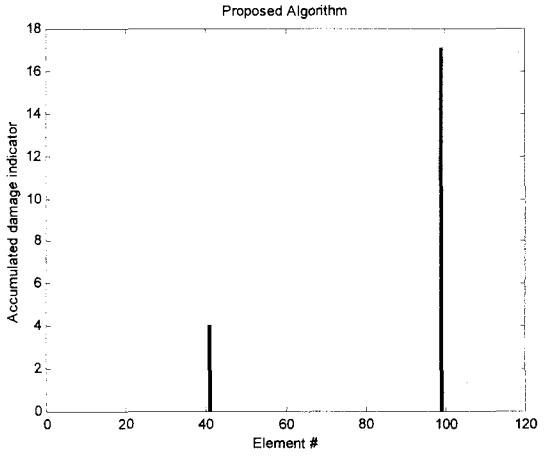

Fig. 12 The proposed algorithm applied to experimental data for cracks at nodes 40 and 90 using freq. range from 307 to 375 Hz.

(2) Using the proposed algorithm

The proposed algorithm is applied using CSD magnitudes in the same frequency range from 307 to 375 Hz. Crack at node 40 was detected and its position is very accurately indicated at element 41. On the other hand, crack at node 90 was detected and its position is indicated less accurately at element 99, as shown in Fig. 12. It is also observed that when damage occurs between sensors, it can be detected at the nearest sensor position. Accumulated damage indicator at element 99 is higher than that at node 41. Damage was detected twice at element 99 and only once at element 41 (Fig. 13).

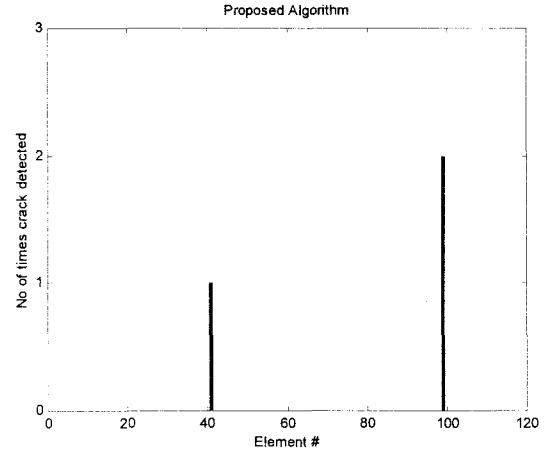

Fig. 13 Number of times cracks detected in experimental data for cracks at nodes 40 and 90 using freq. range from 307 to 375 Hz.

6. Numerical model

The numerical model of the beam was created using Structural Analysis Program[16], SAP2000 (Fig. 14). Shell elements, with the same thickness and material properties of the actual beam are used for the flange and the web. Springs are used to simulate the end fixation of the beam. Spring stiffness values are adjusted until the resonant frequencies of the model are close to the measured experimental frequencies. In order to simulate the actual experiment, the excitation force of the piezoelectric actuator is simulated by a time history function, which contains different frequencies from 0 to 400 Hz. Displacement time history response is measured at seven different points and one more point is used as a reference. CSD is calculated

from displacement response at every sensor relative to the reference channel. Mode shapes are calculated from CSD magnitude at resonant frequencies and the sign is determined from phase angle. Mode shapes calculated directly by SAP2000 were not used. Crack is simulated by removing thin shell element at the crack position. Cubic polynomial is also used to approximate modal amplitude and CSD magnitude between sensors. Therefore, the element numbers of the numerical model and the actual beam are the same.

The first objective of using numerical model is that more mode shapes can be measured than from the experiment and hence the most accurate results using the existing algorithm of Damage Index Method can be obtained. Those results are then compared with the results obtained from the proposed algorithm. The second objective of using the numerical model is to evaluate the feasibility of the proposed algorithm to detect and localize damage in a numerical model of a structure when only data on a low frequency range of vibration is available. Since there is no noise on the data obtained from the numerical model, CSD magnitudes on a very low frequency range will be used on the proposed algorithm.

Three cases of damage are introduced to the numerical model. The first case is single crack, 3 x 45 mm, at node 40, the second case is double cracks at nodes 40 and 80 with the same previous dimensions, and the third case is the same like the first case after increasing the crack length to 90 mm, in order to evaluate the ability of the proposed algorithm to measure the damage increase.

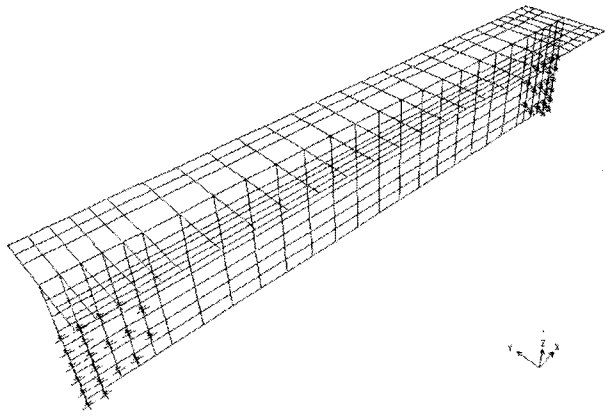

Fig. 14 Numerical model of the beam

7. Damage identification methods applied to numerical data

Damage Index Method is applied to the numerical data for the different cases of damage using the first lower five mode shapes. The proposed algorithm is applied to the numerical data in two stages. In the first stage, CSD magnitudes are measured in a low frequency range, from 4 to 50 Hz, in order to evaluate the feasibility of the proposed algorithm to detect and localize the damage using very low frequency. In the second stage, CSD magnitudes are used in the total frequency range, from 4 to 400 Hz, in order to determine the total number of detecting the crack and the maximum value of accumulated damage indicator.

7.1 Crack at node 40

(1) Using Damage Index Method

Fig. 15 shows the results when the Damage Index Method was applied to detect damage at node 40 and the first lower five mode shapes were used. The position of damage was indicated accurately at element 39 and there was a likelihood of a false positive reading at element 59.

(2) Using the proposed algorithm

When CSD magnitudes were used in the frequency range from 4 to 50 Hz, very accurate results are obtained for detecting the damage at element 40. The damage position at this element was predicted by the proposed algorithm at elements 39 and 38, as shown in Fig. 16. In Fig. 17, damage at element 39 was detected 6 times and damage at element 38 was detected 5 times. Damage was then predicted 11 times using very low frequency range.

Figs. 18 and 19 show the indicated position of damage and number of times of crack detection, respectively, when the total frequency range, from 4 to 400 Hz, was used. At the detected

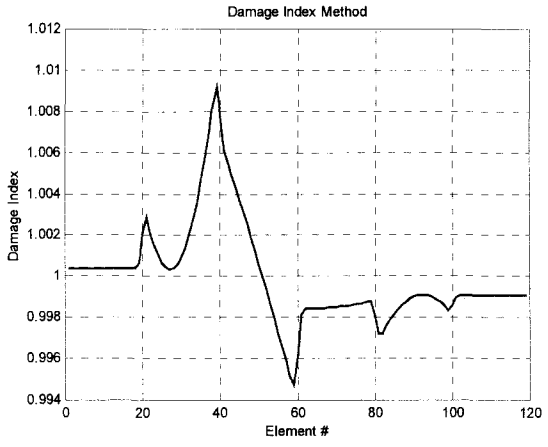

Fig. 15 Damage Index Method applied to numerical data for crack at node 40

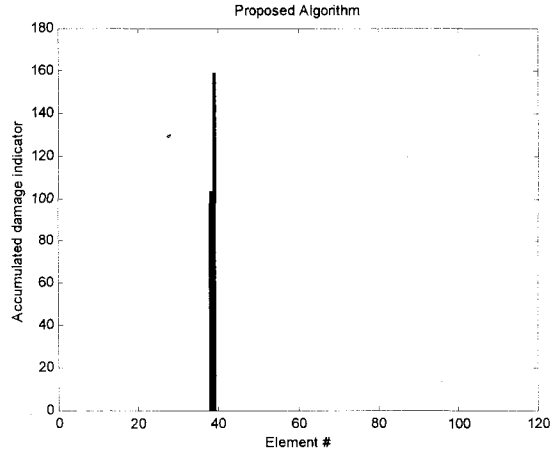

Fig. 16 The proposed algorithm applied to numerical data for crack at node 40 using freq. range from 4 to 50 Hz.

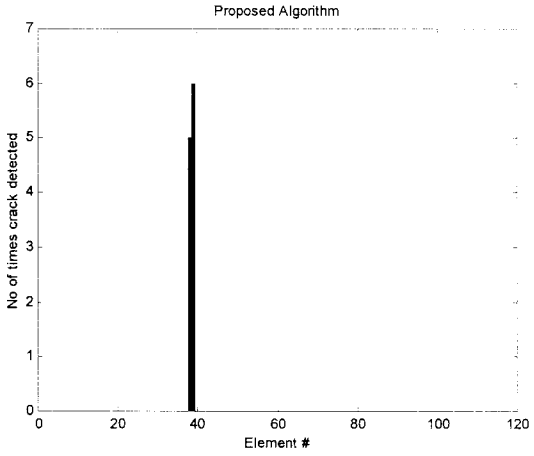

Fig. 17 Number of times cracks detected in numerical data for crack at node 40 using freq. range from 4 to 50 Hz.

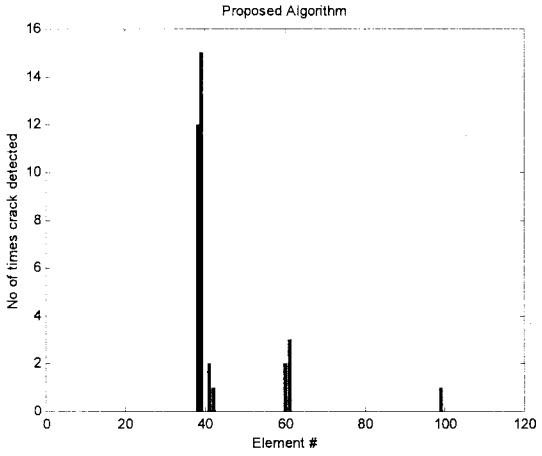

Fig. 19 Number of times cracks detected in numerical data for crack at node 40 using freq. range from 4 to 400 Hz.

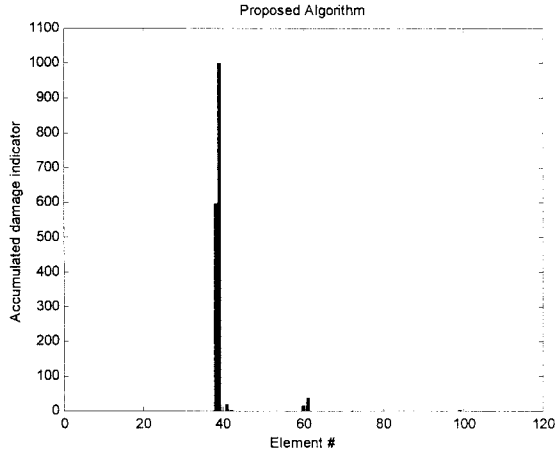

Fig. 18 The proposed algorithm applied to numerical data for crack at node 40 using freq. range from 4 to 400 Hz.

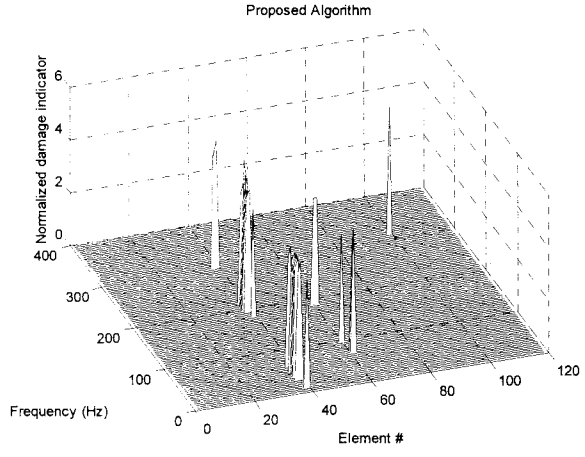

Fig. 20 Predicted position of damage vs. freq. for numerical data and crack at node 40.

elements, 38 and 39, accumulated damage indicator increased tremendously while the corresponding values at elements 60 and 100 (false positive readings) were almost negligible. Damage was indicated 15 times at element 39, 12 times at element 38, twice at element 41, and once at element 42. Two false positive readings were predicted around element 60 (5 times) and 99 (once) but their accumulated damage indicator values were disproportionately small (Fig. 18). Fig. 20 shows the normalized damage index value at each element versus the frequency value at which CSD is measured. From this figure, the following conclusions can be drawn:

(I) Damage at element 40 was indicated accurately when CSD magnitudes were measured in the frequency range, from 12 to 64 Hz, from 184 to 216 Hz and at 300 Hz.

(II) False positive readings were predicted near the actual position of damage when CSD magnitudes were measured at the frequencies 72, 76, 100, and 188 Hz.

(III) False positive readings were predicted far from the actual position of damage when CSD magnitudes were measured at frequency 312 Hz.

(IV) Neither damage nor false positive readings were predicted when CSD magnitudes were measured in other frequency range.

7.2 Cracks at nodes 40 and 80

(1) Using Damage Index Method

In a manner similar to the first case of damage, Damage Index Method was applied using the first lower five mode shapes and the obtained results are shown in Fig. 21. Damage was predicted at element 80 only as indicated by the peak value of damage index at this element and there was no indication of damage observed at element 40.

(2) Using the proposed algorithm

When the proposed algorithm was applied using CSD magnitudes in the frequency range from 4 to 50 Hz, the two positions of damage were detected and localized accurately, as shown in Fig. 22. Accumulated damage indicator value at element 80 is higher than that at element 40. Damage was predicted three times at element 81, once at element 39 and once at element 38 (Fig. 23). Therefore, the proposed algorithm performed very well for the case of multiple

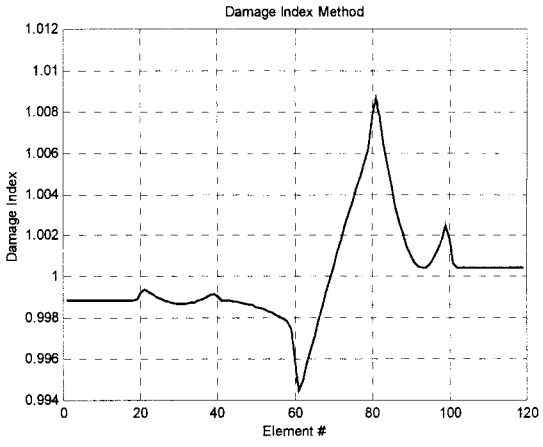

Fig. 21 Damage Index Method applied to numerical data for cracks at nodes 40 and 80.

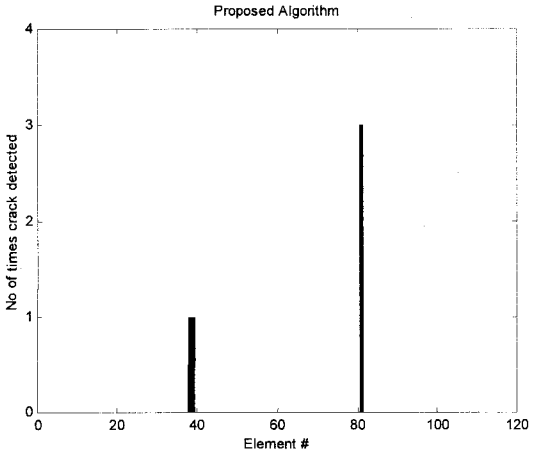

Fig. 23 Number of times cracks detected in numerical data for cracks at nodes 40 and 80 using freq. range from 4 to 50 Hz.

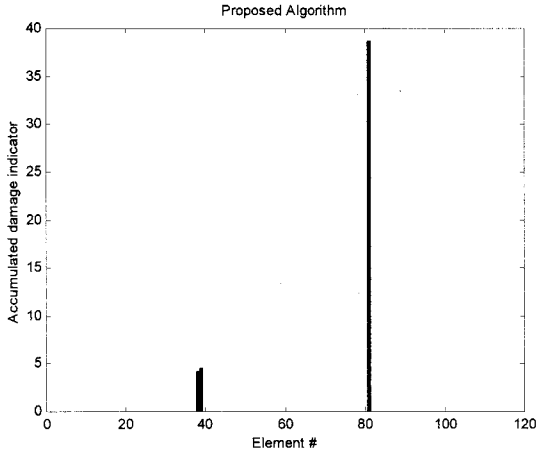

Fig. 22 The proposed algorithm applied to numerical data for cracks at nodes 40 and 80 using freq. range from 4 to 50 Hz.

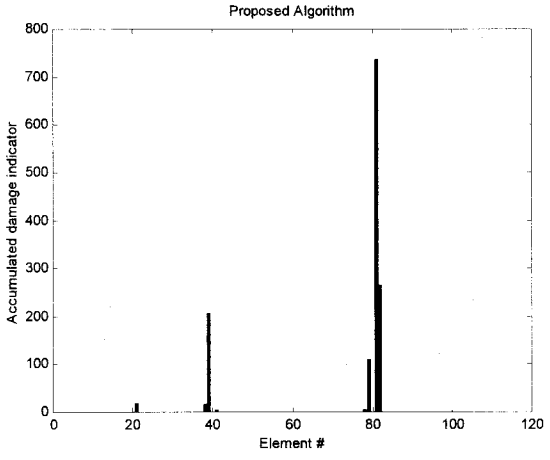

Fig. 24 The proposed algorithm applied to numerical data for cracks at nodes 40 and 80 using freq. range from 4 to 400 Hz.

cracks when very low range of frequency was used. Although the positions of damage are symmetrical, they are not equally predicted; this can be attributed to the position of the reference channel being offset from the centerline of the beam. Figs. 24 and 25 show the results when the frequency range from 4 to 400 Hz was used. Damage at the two positions were predicted and localized accurately. The value of accumulated damage indicator of the false positive reading at element 21 is very small compared to its value around the actual locations of damage at elements 40 and 80. Damage around element 40 is detected 10 times, around element 80 is detected 26 times and around element 20 (false positive reading) is detected only twice. When a wider range of frequency range is used, higher values of accumulated damage indicator are obtained and there is an increase in the number of times the crack is detected, which ensures the accuracy of the obtained results. On the other hand, because experimental data usually contains noise and measurement errors, the use of a wide frequency range is not recommended. Fig. 26 shows the normalized damage index value at each element versus frequency value at which CSD is measured. When Fig. 26 is compared to Fig. 20, the following conclusions are drawn:

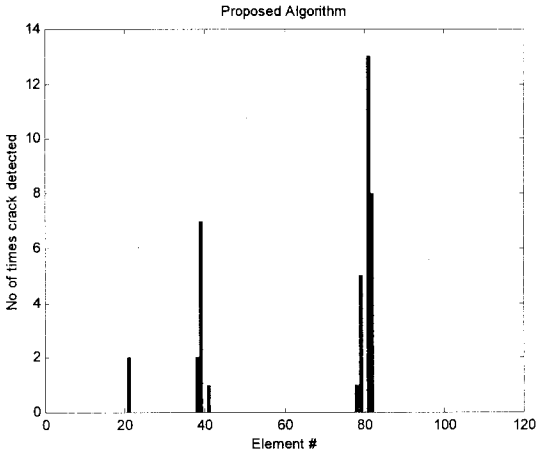

Fig. 25 Number of times cracks detected in numerical data for cracks at nodes 40 and 80 using freq. range from 4 to 400 Hz.

(I) The frequency range, which gave good results for detecting the damage at element 40, has changed after introducing the second crack at element 80.

(II) The false positive readings at elements 60 and 100, which were

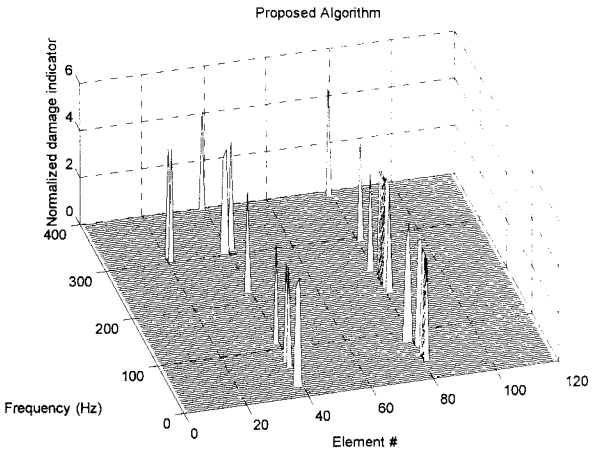

Fig. 26 Predicted position of damage vs. freq. for numerical data and cracks at nodes 40 and 80.

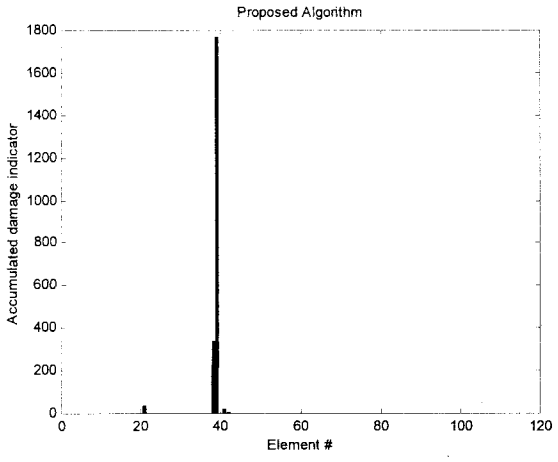

Fig. 27 The proposed algorithm applied to numerical data for crack at node 40 after increasing crack length using frequency range from 4 to 400 Hz.

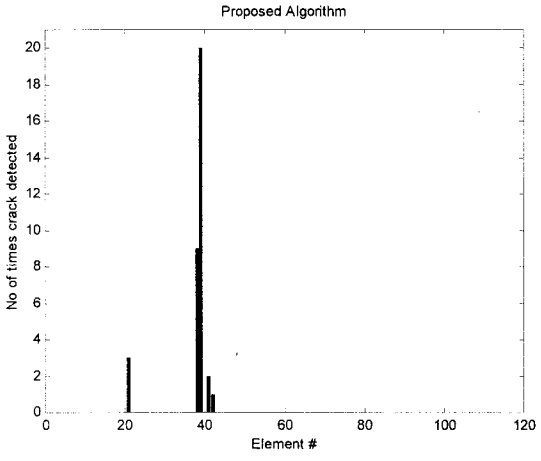

Fig. 28 Number of times cracks detected in numerical data for crack at node 40 after increasing crack length using frequency range from 4 to 400 Hz.

predicted for the first case of damage are not predicted for the second case. The false positive reading at element 21 is predicted for the second case of damage only.

(III) The frequency range giving accurate results to detect damage of element 80 is different from that of element 40.

It can then be concluded that, the effective frequency range differs with each damage position and damage case (single or multiple cracks).

7.3 The proposed algorithm applied to numerical data for crack at node 40 after increasing the crack length

When the proposed algorithm was applied to the numerical data after increasing the crack length at element 40 to 90 mm, the accumulated damage indicator value increased to the value near to 1800 compared to a value of 1000 before increasing the crack length (Figs. 27 and 18, respectively). Therefore, the proposed algorithm can be used to monitor the damage increase although it cannot be used to estimate the severity of damage. Crack at element 39 is detected 20 times after increasing crack length compared to 15 times before increasing crack length and the number of false positive readings decreased after increasing crack length from total of 6 times to 3 times (Figs. 28 and 19, respectively).

8. Concluding remarks

(1) Vibration based damage identification methods can be applied to monitor the integrity of structures in a global way. A proposed algorithm based on changes in CSD magnitude was introduced and applied to detect and locate damage in a steel beam. In a similar manner this method can be applied for continuous health monitoring of bridges for example. A number of sensors can be fixed on the main girders of the bridge, data from sensors can be transformed by wireless methods, and ambient vibration may be used as an excitation source.

(2) The proposed algorithm for damage identification using CSD magnitudes has shown better results in detecting and localizing cracks than Damage Index Method. The proposed algorithm showed very accurate results in detecting damage and localizing its position for experimental and numerical data and for single and multiple cracks.

(3) The proposed algorithm has shown accurate results when very low frequency range was used without the need for measuring higher modes.

(4) The frequency range, in which CSD magnitude will be used for the proposed algorithm, should be chosen carefully for the experimental data. Modal Assurance Criterion can be a useful tool to identify the frequency range in which the data contains less noise and less measurement errors.

(5) Since CSD is measured from acceleration or displacement response without the need for measuring the excitation force, the proposed algorithm can be a good tool for continuous health monitoring of structures using ambient vibration as an excitation source.

(6) The frequency range, which gives good results for detecting damage at certain position, may change when another new crack

exists in another position.

(7) The proposed algorithm can be used to monitor the damage increase although it cannot be used to estimate the severity of damage.

(8) When damage exists between sensors, it is usually predicted at one of the nearest sensor positions. Interpolation using cubic polynomial function to approximate modal amplitude or CSD magnitude between sensors is not efficient for increasing the accuracy of locating damage between sensors. However, interpolation is useful tool to calculate the second derivative of modal data or CSD data.

Acknowledgement

This research is supported by the Grant-in-Aids for Scientific Research, Ministry of Education. The authors wish to express their gratitude for this support. Special thanks to Dr. Inoue and Dr. Sato from Kushiro Seisakusho Co., LTD for their guidance in preparing the specimen.

References

1) Ojalvo, I.U., and Pilon, D., Diagnostics for Geometrically Locating Structural Math Model Errors from Modal Test Data, *Proc. of 29th AIAA/ASME/ASCE/ASC Structures, Structural Dynamics, and Materials Conference*, Williamsburg, VA, 1988.

2) Ricles, J.M., and Kosmatka, J.B., Damage Detection in Elastic Structures Using Vibratory Residual Forces and Weighted Sensitivity, *AIAA Journal*, Vol. 30, No. 9, pp. 2310-2316, 1992.

3) Smith, S.W., and Li, C., A Hybrid Approach for Damage Detection in Flexible Structures, *Proceedings of the 35th AIAA/ASME/ASCE/AHS/ASC Structures, Structural Dynamics, and Materials Conference*, pp. 285-293, AIAA- 94-1710-CP, 1994.

4) Carrasco, C.J. Osegueda, R.A. and Ferregut, C.M. *Modal Tests of a Space Truss Model and Damage Localization Using Modal Strain Energy*, Report FAST 96-10 - FAST Center for Structural Integrity of Aerospace Systems, University of Texas El Paso, El Paso, Texas 79968-0516, July 1996.

5) Peeters B., Maeck J. and De Roeck G., Vibration-based damage detection in civil engineering: excitation sources and temperature effects, *Smart Mater. Struct.* 10, pp.518-527, 2001.

6) Doebling S. W., C. R. Farrar, M. B. Prime, and D. W. Shevitz, *Damage Identification and Health Monitoring of Structural and Mechanical Systems from Changes in their Vibration Characteristics*, A Literature Review, Los Alamos National Laboratory Report, LA-13070- MS, 1996.

7) Farrar C. R. and D. A. Jauregui, *Damage Detection Algorithms Applied to Experimental and Numerical Model Data from the I-40 Bridge*, Los Alamos National Laboratory Report, LA-12979-MS, 1996.

8) E. Kummer, J. C. S. Yang and N. G. Dagalakis, Detection of fatigue cracks in structural members, *2nd American Society of Civil Engineering/EMD Specialty Conference*, Atlanta, Georgia, 445-460, 1981.

9) J. C. S. Yang, J. Chen and N. G. Dagalakis, Damage detection in offshore structures by the random decrement technique, *Journal of Energy Resources Technology, American Society of Mechanical Engineers* 106, 38-42, 1984.

10) R. G. Flesch and K. Kernichler, Bridge inspection by dynamic tests and calculations dynamic investigations of Lavent bridge, *workshop on Structural Safety Evaluation Based on System Identification Approaches* (H. G. Natke and J. T. P. Yao, editors), 433-459, Lambrecht/ Pfalz, Germany: Vieweg & Sons, 1988.

11) S. F. Masri, R. K. Miller, A. F. Saud and T. K. Caughey, Identification of nonlinear vibrating structures, *Journal of Applied Mechanics* 54, 923-929: Part I-formulation, 1987.

12) H. G. Natke and J. T. P. Yao, System identification methods for fault detection and diagnosis, *International Conference on Structural Safety and Reliability, American Society of Civil Engineers, New York*, 1387-1393, 1990,

13) Stubbs N., J. T. Kim, and C. R. Farrar, Field Verification of a Nondestructive Damage Localization and Sensitivity Estimator Algorithm, *Proceedings of the 13th International Modal Analysis Conference*, pp. 210-218, 1995.

14) Oshima T. et al., Study on damage evaluation of joint in steel member by using local vibration excitation, *Journal of Applied Mechanics*, Vol.5, pp.837-846, 2002.

15) Ewins D. J., *Modal Testing: Theory and Practice*, John Wiley, New York, 1985.

16) SAP2000, *Integrated Finite Element and Design of Structures*, Analysis Reference Manual, Computers and Structures, Inc. Berkeley, CA, USA, 1995.

(Received: April 16, 2004)